High-resolution deep-level transient spectroscopy studies of gold and platinum acceptor states in diluted SiGe alloys

K. Gościński and L. Dobaczewski
Institute of Physics, Polish Academy of Sciences, al. Lotników 32/46, 02-668 Warsaw, Poland

K. Bonde Nielsen and A. Nylandsted Larsen
Institute of Physics and Astronomy, University of Aarhus, Ny Munkegade, DK-8000 Aarhus C, Denmark

A. R. Peaker
Centre for Electronic Materials, University of Manchester Institute of Science and Technology, P.O. Box 88, Manchester M60 1QD, United Kingdom

(Received 16 May 2000; revised manuscript received 27 November 2000; published 21 May 2001)

High-resolution Laplace deep-level transient spectroscopy spectra for gold- or platinum-diffused SiGe samples show an alloy splitting that is associated with the alloy fluctuations in the proximity of the defect. For the case of the platinum acceptor state, the effect of the level splitting caused by alloying in the first and also in the second shell of surrounding atoms can be distinguished. For the case of the gold acceptor, only the effect from the first shell of atoms is observable but the manifestation of alloying in the second-nearest shell can be seen as line broadening. We have found that the electronic energy level is affected by alloying in the first-nearest neighborhood by a factor of 2–3 more than by alloying in the second-nearest shell. The absolute values of the energy differences obtained from the Arrhenius plots for different defect configurations agree with those inferred from the peak separations observed in the spectra. A clear preference for gold and platinum to enter substitutional Si sites adjacent to Ge has been revealed. This may be interpreted in terms of an enthalpy lowering as a result of the fact that both metals are able to replace the host silicon atom more easily than the germanium atom in the substitutional position.

DOI: 10.1103/PhysRevB.63.235309 PACS number(s): 71.55.Cn, 61.72.Ji, 68.55.Ln

INTRODUCTION

In semiconductor materials the electronic levels of point defects, which result from the binding of carriers on localized orbits, are sensitive to details of the atomic configuration in their close vicinity. Thermal excitation of such defects results in transitions of carriers from the defect to either the conduction or valence band, i.e., delocalization of carriers. As a result, for semiconductor alloys, the thermal emission process reflects the spatial fluctuations in local alloy composition affecting the initial state of the transition. This is because the alloy fluctuations are well averaged for the final state of the carrier in the band. In these cases the thermal emission spectra obtained by techniques such as deep-level transient spectroscopy (DLTS) may reveal a structure that can be interpreted in terms of ''alloy splitting'' of the bound-state total energy.[1–5]

In ternary semiconductor alloys the alloying effect occurs in every second shell of atoms; thus usually one assumes that only one shell of atoms influences the properties of the ground state of the localized defect. For binary alloys, such as SiGe, one can expect that at least two shells of atoms may influence the electronic properties of the defect; however, the alloy splittings originating from different shells of atoms are not equivalent. Consequently, investigations of the alloy splitting effects for defects in binary alloys can be extremely informative provided the experimental technique offers sufficient resolution to see the effects originating from different shells of atoms.

The resolution of conventional DLTS techniques (defined as the ability to recognize two close emission rates) is at most a factor of 10 in the rate, provided one can perform a reliable and unambiguous line-fitting procedure.[6] In practice the resolution is much worse. This value can be translated into the energy resolution for the activation energy of the thermal emission process. Usually DLTS measurements are performed in a temperature range between 100 and 300 K. This translates as an energy resolution for conventional DLTS measurement ranging between 20 and 60 meV. These values are in most cases insufficient to see the real alloy effects for defects in semiconducting alloys (see the discussion on real and apparent alloy effects observed for the case of the DX centers in $Al_xGa_{1-x}As$ given in Ref. 5).

The emission-rate resolution offered by high-resolution ''Laplace'' DLTS,[7] as used in this study, is much higher than for conventional DLTS. In Laplace DLTS no line-fitting procedure is necessary. This high resolution enables a uniquely detailed mapping of environmental effects on deep centers within dilute SiGe. We show that emission spectra obtained for the platinum and gold acceptor states display a fine structure that can be interpreted as the effect of alloy splitting in terms of the relative number of silicon and germanium atoms in the immediate proximity of the transition metal. Both defects have been studied previously in great detail for pure Si,[8,9] and some conventional DLTS results are available for SiGe alloys.[10–12] For the case of platinum we are able to recognize the alloying effects originating from the first and

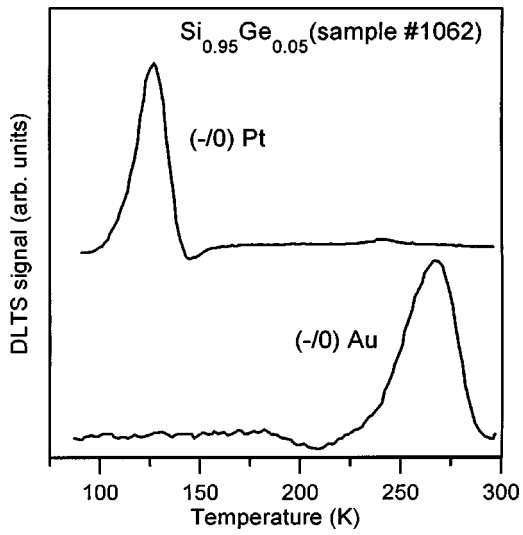

FIG. 1. Conventional DLTS spectra for electron emission from an *n*-type $Si_{0.95}Ge_{0.05}$ crystal diffused with platinum (upper curve) and gold (lower curve). In both cases one featureless line related to the acceptor state for each of the metals is observed.

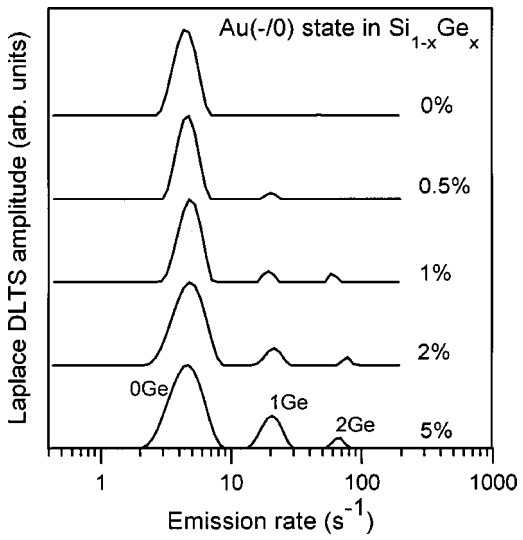

FIG. 2. Laplace DLTS spectra of gold-diffused samples having different germanium content. For each of the spectra the main lines have been aligned and normalized to the spectrum for the 5% sample according to the procedure described in the text.

second shells of atoms while for the case of the gold acceptor state the influence of both shells on the emission is observed indirectly. We further show by analyzing the relative concentrations of different local alloy configurations that both transition metals display a preference for sites next to Ge when they are diffused into the alloy.

SAMPLES

Most of the samples used in this study were grown by molecular-beam epitaxy on (100) Si substrates. The alloy composition of the active layer of $Si_{1-x}Ge_x$ (4 μm thick) was 0, 0.5, 1, 2, or 5 at. %. Between the active layer and the substrate compositionally graded buffer layers were grown in order to accommodate lattice-mismatch strain and reduce the number of misfit dislocations (see Ref. 13 for details of the growth procedure). Samples grown according to this procedure are known to have a low density of dislocations ($<10^5\,cm^{-2}$) and a low concentration of deep levels ($<10^{12}\,cm^{-3}$). The uniform active layers were *n* type, doped with $5\times10^{15}\,Sb\,cm^{-3}$. Both p^+n-mesa and Schottky diodes were used in this study. The dopant metals (either Pt or Au) were diffused into the layers at 800 °C for 24 h. In the case of the mesa diodes this was done through the p^+ layer and in the case of the Schottky diodes prior to diode formation.

Figure 1 shows conventional DLTS spectra for two samples prepared from the same $Si_{0.95}Ge_{0.05}$ crystal. One sample was diffused with gold and the other with platinum. In both cases one peak is observed on each of the spectra, which can be attributed to the well-known acceptor states of the transition metals in the substitutional positions. Although the sample active layers are prepared from a semiconductor alloy no structure is observed within the peaks of these spectra.

RESULTS AND DISCUSSION

Alloy splitting effect for gold and platinum

Figures 2 and 3 show Laplace DLTS spectra for gold and platinum acceptors in SiGe alloys with 0–5% of Ge, respectively. The spectra have been normalized in terms of the magnitude and emission rate of the 0Ge line. This enables a direct comparison to be made between the various samples. Some of the spectra for a given impurity have not been measured at exactly the same temperatures, and the alloying alters the band gap of the semiconductor, which causes a shift

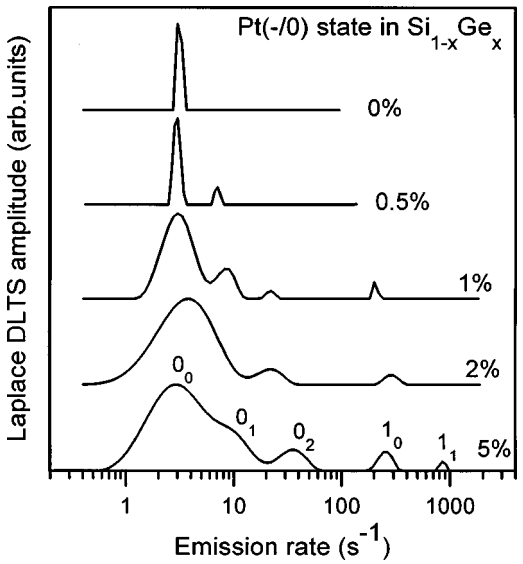

FIG. 3. Laplace DLTS spectra of platinum-diffused samples having different germanium content. For each of the spectra the main lines have been aligned and normalized to the spectrum for the 5% sample.

of the main features on the spectra so that they cannot be overlaid without normalization. The emission process has an activation character, i.e., is governed by the formula

$$e_n = A \exp(-E_n/kT), \tag{1}$$

where E_n is the activation energy for thermal emission, T is the measurement temperature, k is the Boltzmann constant, and A is a constant. Note that the constant A contains other defect parameters like the capture cross section and the entropy term; however, for visualization of differences between different local alloy configurations we assume that any changes in the defect capture cross section and entropy are hidden in changes of the activation energy of the emission. Moreover, in the general case the preexponential factor should depend on the temperature as T^2. When the Laplace DLTS spectra are taken at different temperatures for the Arrhenius type of spectral analysis this T^2 dependence is explicitly used.

In Figs. 2 and 3 the spectra have been shifted horizontally in order to align the main peak of each spectrum. When the spectra measured at two different temperatures T_1 and T_2 are compared, the horizontal axis for each of the spectra has to be recalculated according to the formula $\ln[e_n(T_2)] \approx (T_1/T_2)\ln[e_n(T_1)]$, which is a direct consequence of Eq. (1). This formula is valid as long as T_1 is not too far from T_2; otherwise a consideration of the T^2 term in the constant A becomes necessary. This recalculation procedure compensates for the fact that the Laplace DLTS spectrum for a given sample covers a wider range on the frequency scale when it is taken at a lower temperature than at a higher temperature (the resolution of the method is proportional to the temperature).

When the germanium content in the crystal increases additional features in the Pt- and Au-related Laplace DLTS spectra appear on the high-frequency side of the main line. A simple analysis of the conventional DLTS line shape allows us to conclude that these features can cause a broadening of the conventional DLTS peak on the low-temperature side. This will happen if the emission rate differs from the emission rate of the main line by less than a factor of 4 and the amplitude is larger than 50% of the main-line amplitude. Figure 2 and Table I(a) show that for the case of the gold acceptor state these conditions are not fulfilled and the conventional DLTS peak seen in Fig. 1 is not significantly broadened although a small shoulder on the low-temperature side is observed. For the case of the platinum acceptor the additional features are less well separated on the emission-rate scale, so that the conventional DLTS line in Fig. 1 is broadened with respect to the line observed in the pure silicon sample.

Clear trends are seen on the spectra in Figs. 2 and 3 for both impurities which allow us to associate the features resulting from increasing germanium content with different local configurations of the alloy in the vicinity of the metal atom.[14] Figure 4 shows a schematic flat diagram of the random alloy (for 5% of Ge) in the first- and the second-nearest neighborhood of the defect. The light gray bar diagram represents probabilities of finding the alloy configuration having 0, one, or two of four germanium atoms (assigned here as 0Ge, 1Ge, and 2Ge, respectively) in the first shell of atoms. When the second shell of atoms is taken into account these lines split into subsets which are depicted by dark gray bars. The lines in these split sets are now marked by figures with subscripts, where the figures and subscripts refer to the number of germanium atoms in the first- and second-nearest neighborhood, respectively.

TABLE I. Relative concentration of different local environment configurations for (a) gold and (b) platinum acceptors in SiGe alloy compositions. ''Theoretical'' values inferred from an analysis of a perfectly random alloy (see diagram in Fig. 4) are compared to ratios of peak amplitudes assigned to the Laplace DLTS spectra. The lines not observed in the spectra are marked n/o.

Composition (% of Ge)	Theory	Experiment	Theory	Experiment
	(a)Au normalized to 0Ge			
	1Ge $(1_0+1_1+\cdots)$		2Ge $(2_0+2_1+\cdots)$	
0.5	0.020	0.06 ± 0.03		n/o
1	0.043	0.08 ± 0.03		
2	0.078	0.13 ± 0.04	0.002	
5	0.21	0.30 ± 0.04	0.015	0.05 ± 0.03
	(b) Pt normalized to 0_0			
	0_1		1_0	
0.5	0.062	0.10 ± 0.05	0.020	n/o
1	0.12	0.21 ± 0.05	0.042	0.03 ± 0.02

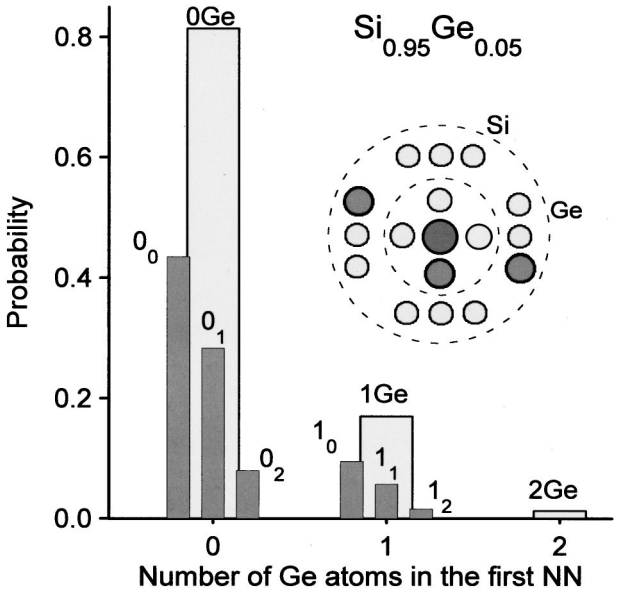

FIG. 4. Flat diagram of the SiGe alloy showing two shells of atoms surrounding the metal impurity. The light gray bars show probabilities of finding a given number of germanium atoms in the first-nearest neighborhood of the metal for the random alloy having 5% of germanium. These lines split into subsets (dark gray bars) if one assumes that the second-nearest neighborhood plays a role.

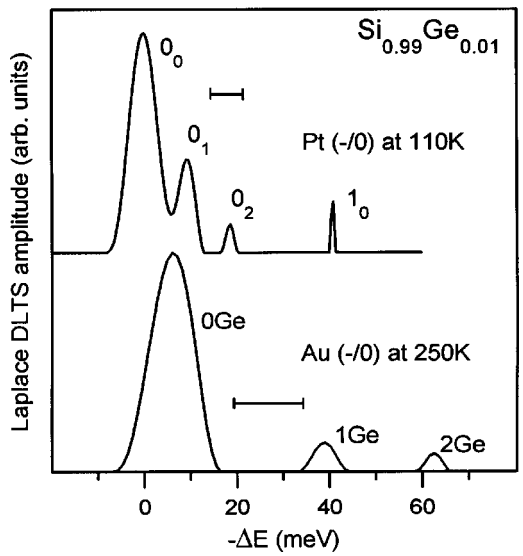

FIG. 5. Two Laplace DLTS spectra for the platinum and gold acceptor states in $Si_{0.99}Ge_{0.01}$, where the emission-rate scale has been recalculated as an energy-difference scale using formula (1). See text for details.

A comparison of the diagrams for 5% of Ge in the alloy-with the spectra for the corresponding alloy leads to the conclusion that the structure seen on the spectra is a manifestation of the alloying, where only the role of the first-nearest neighbors is apparent for the case of gold, while the influence of the first and second neighbors can be seen in the thermal emission process for the case of platinum. The peak assignments for the spectra in Figs. 2 and 3 and the diagram from Fig. 4 are the same. Note that the Laplace DLTS spectra shown for the 5% samples in Figs. 2 and 3 correspond to the conventional DLTS spectra shown in Fig. 1 for the same samples. Similar bar diagrams can be constructed for other alloy compositions, reproducing tendencies in particular alloy configuration concentrations. For alloy compositions above 5% (samples with the germanium content up to 25% have been checked) the thermal emission becomes less well defined with many contributing features, which makes the numerical procedures for the calculations of the Laplace DLTS spectra unstable and inconclusive.

Equivalency of the alloy effect for both impurities

Figure 5 shows two Laplace DLTS spectra of the gold and platinum acceptors in a SiGe alloy with 1% Ge. These measurements were carried out at different temperatures; however, for direct comparison of the spectra the frequency scale has been converted to an energy-difference scale using a modification of the formula (1), $\Delta E = -kT\ln(e_n/e_{n0})$, where e_{n0} is an arbitrary reference frequency. Note that in this figure larger energy values mean a decrease of the activation energy for the emission, i.e., a faster emission process. Such a presentation of the spectra allows a direct comparison of the influence of the alloy on the defect energy levels irrespective of some aspects of the experimental conditions, in this case the temperature of the measurement.

It is seen that when the center of gravity of the three left-hand-side lines seen for the platinum spectrum is aligned with the center of gravity of the 0Ge line of the Au spectrum, the right-hand-side line of platinum aligns with the 1Ge line of gold. This means that in both cases the alloy splitting of the energy level caused by a replacement of one silicon atom among the first-nearest neighbors of either the gold or the platinum by germanium is around -35 meV. For the case of platinum a similar change in the second-nearest neighborhood results in a change in the defect energy by approximately -10 meV.

The spectra for the gold acceptor depicted in Fig. 2 clearly show that the main 0Ge line broadens with increase of the Ge content but never splits into components as observed for the case of platinum. In order to understand this observation one should remember that the energy resolution of the Laplace DLTS technique is almost inversely proportional to the temperature at which the spectrum is taken. This means that the platinum spectrum was obtained with a factor of 2.5 higher resolution than the gold spectrum. As a result, an additional splitting of the gold 0Ge line is revealed in the platinum case. The error bars in Fig. 5 show the energy resolution for both spectra when an emission-rate resolution (understood here as the ability of the numerical methods to distinguish two emission rates) differing by a factor of 2 is assumed.

On the other hand, one could expect that although the 0Ge line cannot split it should become asymmetric when the Ge content increases. This effect is not observed in the spectra shown in Fig. 2. We explain this lack of expected asymmetry for the 0Ge line as a manifestation of limitations of the Tikhonov regularization method which we use for the Laplace transform inversion.[16] This method allows us to find good approximations for the Laplace spectrum with a clear resolution limit. When two features in the spectrum differ in emission rate by less than the resolution limit of the method (a factor of around 2) the Tikhonov method will show these features as one broad and *symmetric* line. However, if the line separation is larger than the resolution limit then the line starts to be truly asymmetric; sometimes it splits, sometimes a small shoulder on the strong line appears depending on the noise level. Problems related to the Tikhonov regularization method resolution and the role of noise there have recently been reviewed by Istratov and Vyvenko in Ref. 17.

Defect ionization enthalpies

The diagram shown in Fig. 5 enables the differences between apparent activation energies for different defect configurations to be evaluated. This evaluation is based on formula (1) where it is assumed that the carrier capture cross sections [hidden in the constant A of Eq. (1)] for these configurations do not depend on the local alloy composition. It is not necessary to make this assumption when the energy difference is evaluated from the absolute values of the activation enthalpies. The conventional DLTS procedure is to find these values from Arrhenius plots, i.e., from the $\ln(e_n/T^2)$ versus $1/T$ dependence. If the Laplace DLTS measurements are performed on defects producing rather broad spectra this procedure, although in principle possible, has limited applicability. In order to construct a conclusive Arrhenius plot it is necessary to observe a stable Laplace spectrum over a

significantly wide temperature range. The high-temperature limit for an Arrhenius-type analysis is reached when spectral features having the fastest emission rates start to approach the highest measurement frequency of the experimental setup. The low-temperature limit is reached when the emission rate for the slowest features in the spectrum is so low that the transient averaging procedure no longer reduces the experimental low-frequency noise coming from the temperature fluctuation, $1/f$, or the power line. As a result of the increase of the total noise the Laplace DLTS method loses resolution. Consequently, the broader Laplace DLTS spectrum has a narrower temperature range available for an Arrhenius-type analysis than a δ-function spectrum.

For gold and platinum acceptor states in SiGe diluted alloys the Arrhenius type of emission-rate analysis brings another complication. Although it could be expected that for low germanium content the Laplace DLTS spectra would be narrower and more advantageous for the observation of different component emission rates over a wide range of temperatures, the amplitudes of these components are small as a result of the low germanium content. In some cases this makes the Laplace DLTS spectrum unstable at extreme temperatures, which again narrows the possible range of temperatures available for observation of these small features. As a result, in the Laplace DLTS experiment it is much easier to obtain a spectrum demonstrating the relative differences between the features in the spectra than to evaluate the absolute values of the ionization enthalpies. In the first case the sample temperature and the data acquisition parameters can be optimized specifically for each particular sample in order to obtain the best signal-to-noise ratio—a consideration essential for stable Laplace DLTS spectra. The results obtained for gold and platinum in cases where the Arrhenius type of analysis was possible are gathered in Tables II(a) and II(b). Figures 6 and 7 show the Arrhenius diagrams for some gold- and platinum-diffused samples.

For the 5% sample the ionization enthalpies for the 0Ge and 1Ge lines (580 ± 20 and 550 ± 40 meV, respectively, as shown in Fig. 6) are consistent with the spectra shown in Fig. 2, i.e., the defect configuration having slower emission rate is characterized by a larger activation energy for the emission process. For this sample the horizontal axis of the Laplace DLTS spectrum can be converted to an energy scale as in Fig. 5. This allows the relative difference of the activation energies to be evaluated. For these two configurations it is around 35 meV, which is consistent with the difference in the two enthalpies, keeping in mind the standard deviations for these two values.

The spectra observed for the platinum acceptor case constitute a much less favorable situation for performing an Arrhenius-type analysis. They are much broader with more features—a situation that reduces the available temperature range for measurements. For the 0.5% and 1% samples, besides the main 0_0 line, the subsidiary 0_1 line could be analyzed, and also the 1_0 line for the 1% sample. The absolute energy separation for the 0_0 and 1_0 lines in the 1% sample (see Fig. 7) is consistent with the value obtained from Fig. 5. In addition, the difference between the enthalpies for the 0_0 and 0_1 lines for the 0.5% and 1% samples agrees satisfactorily, at least in the energy trend, with the estimate obtained from the peak separation for the spectrum shown in Fig. 5. The 2% sample was not as high quality as the other layers and consequently we have only been able to construct an Arrhenius plot for the main line. For the sample with 5% of germanium the spectra become too broad, which again makes the Arrhenius plots inconclusive for other then the main lines.

TABLE II. Thermal emission activation energies (in meV) for the main and some subsidiary lines in the Laplace DLTS spectra for (a) gold and (b) platinum acceptors in different SiGe alloy compositions. The lines not observed in the spectra are marked by n/o.

(a)

Composition (% of Ge)	0Ge	1Ge
0	547 ± 2	n/o
0.5	548 ± 8	
1	550 ± 10	
2	543 ± 7	
5	580 ± 20	550 ± 40

(b)

Composition (% of Ge)	0_0	0_1	1_0
0	225 ± 4	n/o	n/o
0.5	231 ± 1	220 ± 20	n/o
1	221 ± 3	219 ± 10	190 ± 30
2	262 ± 30		
5	255 ± 20		

Equivalency of Laplace and conventional DLTS measurements on Au and Pt acceptor states in SiGe

The Laplace DLTS technique allows one to observe individual local alloy configurations around the central atom of

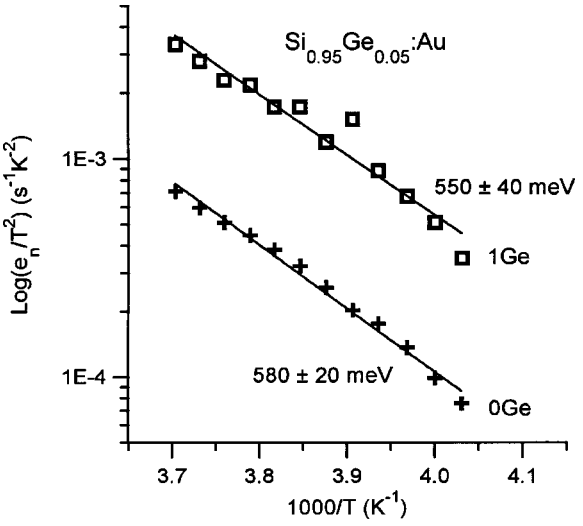

FIG. 6. Arrhenius plot for the 0Ge and 1Ge lines observed in the gold-diffused $Si_{0.95}Ge_{0.05}$ sample.

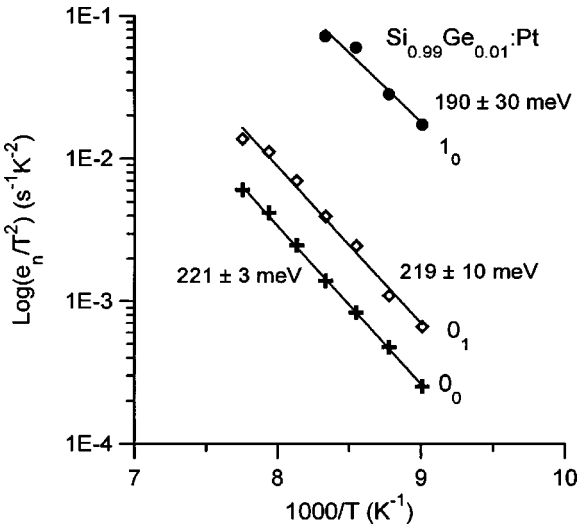

FIG. 7. Arrhenius plot for the 0_0, 0_1, and 1_0 lines observed in the platinum-diffused $Si_{0.99}Ge_{0.01}$ sample.

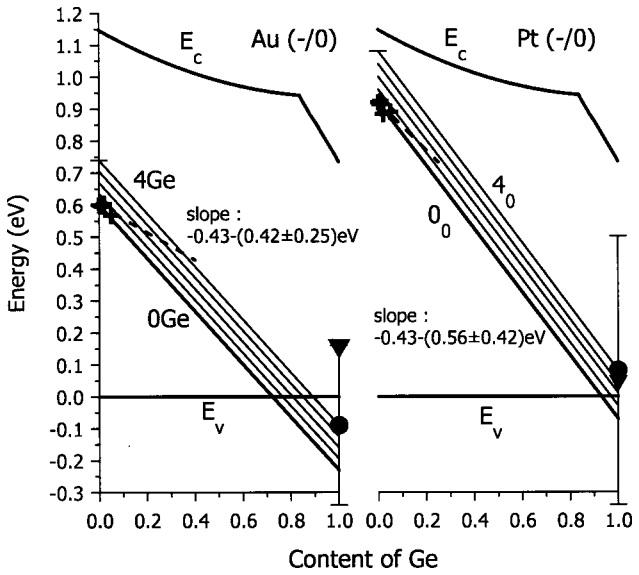

FIG. 8. The measured ionization enthalpies for the 0Ge configuration of Au and the 0_0 configuration of Pt (crosses) overlaid on the SiGe conduction-band variation, where all changes are related to the top of the valence band (according to Ref. 18). The full circles with the error bars show the positions of both acceptor states when the observed values from the 0–5 % alloy range are extrapolated to pure germanium. The triangles are the corresponding values measured in Ref. 19. See text for details.

the defect. However, at least for the elemental semiconductor alloys, this method gives conclusive results only for diluted alloys where there is a limited number of configurations contributing to the signal. On the other hand, the conventional DLTS technique does not suffer from this limitation, and the results obtained for both acceptor states in a wider range of alloys are available.[10–12] Conventional DLTS measurements performed on alloys provide an energy level that is an unresolved convolution of all the levels originating from different alloy configurations and thus it is important to compare results from these two techniques.

A standard linear-regression analysis has been performed for the data presented in the first column of Table II. The reciprocal values of the standard deviations of individual values have been used as their weights. From this procedure it is concluded that the activation energy for emission from the Au acceptor state 0Ge configuration increases with increasing Ge content with the rate $dE_n/dx = 0.42 \pm 0.25$ eV. The same analysis for the Pt acceptor state 0_0 configuration gave 0.56 ± 0.42 eV. Figure 8 shows measured energies for both configurations (crosses) overlaid on the SiGe conduction-band variation, where all changes are related to the top of the valence band. The above alloy coefficients are increased by the initial slope of the conduction band, equal to 0.43 eV. The changes of the bottom of the conduction band as a function of the alloy composition have been taken from Ref. 18.

In Fig. 8 the alloy dependency inferred from the linear-regression procedure for the 0–5 % alloy composition range is extrapolated throughout the whole range of alloy compositions (thick solid line). For the diluted alloys it is observed that there are no systematic changes in the energy differences between individual configurations. For the sake of this analysis it has been assumed that these differences are constant in the whole range of alloy compositions. As a result, above the lines corresponding to the measured configurations there are parallel lines (thin solid) representing more germanium-rich configurations, i.e., 1Ge, 2Ge, etc. for Au, and 1_0, 2_0, etc. for Pt. The line separations are 35 and 40 meV for Au and Pt, respectively. The full circles are the energies of the $(-/0)$ acceptors for both metals in pure germanium inferred from the above analysis. The error bars for the circles are the uncertainties resulting from the standard deviations of the measured alloy coefficients. Note that for the platinum case this should be the extrapolation of the 4_{12} line which points at the acceptor state in pure germanium. If the separation between 0_0 and 0_1 lines is around 10 meV the line 4_{12} should be 120 meV above the 4_0 line. Actually, a modification of the 4Ge line should also be applied as this line contains unresolved $4_0, 4_1, \ldots, 4_{12}$ lines. The full triangles are the single-acceptor states of both metals in pure germanium measured by Pearton using conventional DLTS.[19]

Despite the large errors there is an obvious correspondence between our measurements performed for low-germanium-content alloys and the energy levels known for pure germanium. One can also conclude from this analysis that in germanium-rich SiGe alloys the 4Si and 3Si (analogs of 3Ge and 4Ge) and some other silicon-rich local configurations of both metals might not be observed, as from this analysis they are expected to be resonant with the valence band.

Gold and platinum siting preferences in the SiGe alloy

The individual peaks on the spectra shown in Figs. 2 and 3 are associated with local alloy configurations that are based on the pattern of peaks inferred from the diagram shown in Fig. 4. While the positions of the peaks on the emission-rate scale show how the electronic properties of the defect are

modified by alloying effects, the relative amplitudes of the peaks provide us with data that can be interpreted in terms of the concentrations of particular local alloy configurations. These amplitudes, when compared to a model of a perfectly random alloy, demonstrate deviations from a random distribution of the metals in the SiGe lattice.

Table I shows a comparison of relative peak amplitudes with those expected for a random alloy. These amplitudes are normalized to the amplitude of the 0Ge line for the case of gold and to the 0_0 configuration for platinum for each alloy composition. The experimental values have been obtained from many spectra taken under different experimental conditions with the errors obtained from a standard statistical analysis of these sets. It should be noticed that a general trend seen in the data presented in Table I is that the observed relative amplitudes of peaks are somewhat larger than expected for a perfectly random alloy. For the case of platinum in samples with larger alloy compositions the Laplace DLTS peaks are not so well separated; consequently, although a general trend is seen, it is difficult to obtain unambiguous quantitative results.

Moreover, for a lower content of germanium in the crystal the expected theoretical values of the peak amplitudes are of the order of 1% of the amplitude of the main line. These small signals are very difficult to quantify in terms of relative magnitude because of the limitations of the Laplace spectrum calculations in the presence of a much larger signal (0Ge) and experimental noise, as discussed previously.

The data presented in Table I show that during diffusion at 800 °C both metal atoms prefer to occupy sites in the lattice next to germanium. For the case of gold we conclude that on average the relative concentration of the 1Ge configuration is approximately twice as big as would be expected for random siting. The site preference of gold can be translated to an estimate of the enthalpy difference between the 0Ge and 1Ge configurations of $\Delta H_{\mathrm{conf}} = kT(800\,^{\circ}\mathrm{C})\ln(2) \cong 60\,\mathrm{meV}$ (disregarding terms other than configuration entropy). However, for the case of platinum such an overpopulation effect for the germanium-rich sites is clearly seen only for the second-nearest-neighbor configuration.

Conventional DLTS measurements do not distinguish particular local configurations; they are averaged. One can assume that these configurations contribute to the conventional DLTS line proportionally to their abundance in the crystal. If these concentrations are governed by a binomial distribution then the average value of any defect parameter should be proportional to the alloy composition. Consequently, the average acceptor energy level in the SiGe band-gap diagram should be a line joining the energy of 0Ge in Si with that of 4Ge in Ge. The dashed lines in Fig. 8 are the average acceptor level energies of both metals measured by Mesli, Kringhøj, and Larsen[11,12] using conventional DLTS. Mesli *et al.* did not specify the standard deviations of their slopes; however, these measurements were performed in a wide range of alloy compositions and thus we can expect that they are quite accurate. When the dashed lines are extrapolated to pure germanium we get values above the real energies measured in germanium for both metals (full triangles in Fig. 8). This observation means that in the 0–30 % range of alloy compositions the measured average energy levels of both acceptors are above the expected average levels for a perfectly random alloy. Our results show that in a given alloy composition for a more germanium-rich local configuration the total energy level increases (see Fig. 8). As a result, the deviation of the measured average energy from the theoretical one can be caused by the fact that the more germanium-rich local configuration concentrations are larger than the ones for a perfectly random alloy. This conclusion agrees again with our observation that for both metals there is a preference to be sited in a more germanium-rich local environment.

This relative overpopulation of sites close to germanium has been related to details of the microscopic mechanism of the diffusion of both metals in silicon by us in a previous publication.[14] It has already been well established that they diffuse by a kick-out process. The diffusion proceeds as the metal impurity switches between an interstitial position and a substitutional position. The switching is accompanied by the movement of a host atom from the substitutional to the interstitial site. The driving force for the accumulation of substitutional Au or Pt is the removal of the self-interstitial atoms by sinks. This process seems to be easier for silicon than for the larger germanium atom. Moreover, it would be expected that due to elastic interactions it is harder to create a pseudo-self-interstitial center (a germanium atom in the silicon host) than a self-interstitial defect (a silicon atom in the silicon host). On the other hand, it is easier for germanium to break the longer and softer Ge-Si bonds during the creation of the pseudo-self-interstitial defect than it is for the corresponding process involving only silicon atoms. The interplay of these competing energy terms during diffusion results in a preference for the metal atoms to reside on Si-substitutional sites close to Ge.

Possible influence of the recombination-generation character of the gold acceptor on the Laplace DLTS spectra

According to the Shockley-Hall-Read theory[15] a mid-gap defect can emit both carriers, i.e., electrons to the conduction band and holes to the valence band, with comparable probabilities. The DLTS technique always measures the sum of these emission rates, i.e., $e_n + e_p$, which results in the rates for a near-mid-gap state being overestimated. For the same reason the DLTS signal amplitude is underestimated as it is multiplied by the term $e_n/(e_n+e_p)$ (see, e.g., Ref. 12 for details). If the germanium content of the sample increases then the gold acceptor level will approach the middle of the band gap, making the hole emission process for all the local alloy configurations more pronounced. Among these configurations the ones having an energy level closer to the valence band should exhibit this effect more strongly. For SiGe alloys conventional DLTS measures an average gold acceptor level and its interaction with the valence band is seen as an apparent decrease of the conventional DLTS peak amplitude for larger Ge content.[12]

Our studies were performed on crystals with low Ge content and in consequence this effect is less important than in

the cases reported in Ref. 12. However, if the hole emission has a measurable role it should manifest itself predominantly for the 5% alloy and for the 0Ge local configuration because the energy level of this configuration is the closest to the valence band. This effect, if present, could be observed in two ways.

First, if the contribution of the hole emission to the observed overall emission process for the 0Ge configuration cannot be neglected then the emission rate should equal $e_n + e_p$ rather than e_n. The 0Ge peak should thus be shifted toward higher emission rates. This shift should not be observed for the 1Ge configuration as in this case the interaction with the valence band is expected to be much weaker. However, in the Laplace DLTS spectra this shift of the 0Ge peak is not observed because the emission-rate ratios between the 0Ge and 1Ge configurations for the 0.5% (considered here as a reference) and 5% alloys are virtually the same. Moreover, the emission-rate ratio between the 0Ge and 1Ge configurations for the 5% alloy is almost the same as for the 1Ge and 2Ge configurations in the same crystal, suggesting that the emission rate for 0Ge is not enhanced by any contribution of the hole emission process, at least within the accuracy of the numerical methods employed for the Laplace spectra calculations.

Second, the amplitude of the 0Ge configuration peak in the 5% alloy should be smaller than expected, i.e., than one can infer from the binomial distribution of the local configurations in a perfectly random alloy. This could be interpreted as an overpopulation of the germanium-rich local configurations around the gold atom in the SiGe matrix. However, this alleged overpopulation should not be observed for other lines and alloy compositions as the interaction with the valence band should be much weaker for all these remaining cases. In the Laplace DLTS spectra this overpopulation effect was observed for all samples studied (see Table I) and also for the 2Ge line in the 5% alloy, and thus cannot be a feature of only one peak in one alloy composition.

The value of the hole emission rate can be estimated from the calculated accuracy of the position of the peak center of gravity on the emission-rate scale in the Laplace DLTS spectrum. The error of the peak emission rate depends, in general, on the noise of the measured signal, but typically is smaller than 10% of the calculated value. Actually, all of the numerical methods used for the Tikhonov regularization method[16] calculate the value of the average emission rate for a given peak more precisely than the peak amplitude. Consequently, if the hole emission rate is hidden in the emission-rate error, then the peak amplitude is also underestimated by around 10%. In practice this amplitude underestimation should relate only to the 0Ge line in the 5% alloy, and consequently it should give the wrong normalization value for the relative peak amplitudes detailed in Table I(a) for this alloy. On the other hand, a simple comparison of theoretical and experimental ratios for 1Ge and 2Ge lines also shows overpopulation of the 2Ge line configuration concentration in respect to the 1Ge concentration; this approach is free from any incorrect normalization resulting from an underestimated concentration of 0Ge.

Problem of a universal defect reference level in alloys

There are a number of different theories that attempt to define a universal reference energy level for semiconductors.[20] Such a level could be used for prediction of the conduction- and/or valence-band discontinuities in band-gap engineering of heterojunctions or Schottky barrier parameters. Usually the theories are tested by using values of the hypothetical reference level for unalloyed semiconductor materials and interpolated for alloys. This avoids unresolved alloy effects. However, band-gap engineering rarely uses heterojunctions made from pure elemental or binary semiconductors but employs their alloys. Some of the theories link the universal reference level to the defect energy level related to a transition-metal impurity (see, e.g., Ref. 21).

The universal defect energy level is defined here as the energy of the defect whose ground-state energy level is not subjected to any alloying effects. For thermal emission from such a level only the final state of the transition would experience the alloying effects, but these would be identical to those for the bands. For the case of both acceptor levels considered in this study it would mean that we are looking for a defect configuration that is not disturbed by alloying, i.e., the case where no germanium atoms can be present as either first- or second-nearest neighbors.

As discussed above, defects in alloys do not have a unique energy level related to the ground state. If an attempt is made to discuss evolution of the ground-state energy level as a function of the alloy composition, it is necessary to keep in mind that in reality one deals with a convolution of contributions to the level from different local configurations of the alloy. As a result, it is possible to talk about the alloy composition dependence of the defect energy level, provided only the energy state related to one alloy configuration for different alloy compositions is observed. A natural choice for such a level would the ''no germanium'' configuration (0Ge or 0_0 configurations, according to our notation) for alloys having a low germanium content. These ''no germanium'' lines for gold and platinum would constitute true reference levels showing how their energy separation from, in this case, the conduction-band edge, changes with alloy composition.

For the case of gold the 0_0 line is not observed unambiguously in any of the samples due to the fact that at the necessary measurement temperature the method has insufficient resolution. What we assigned in this case as the 0Ge line is in reality a convolution of the 0_0,0_1,0_2, etc. lines. In Fig. 2 it is seen that the 0Ge line broadens for increasing germanium content, which clearly shows that the second-nearest neighbors, although not resolved as separate entities, play a role here. As a result, the 0Ge line is not the best candidate for the reference level for gold due to unknown contributions from the second-nearest neighbors. For the case of platinum, the 0_0 line has been observed as a separate line only in the 0.5% and 1% samples, and their enthalpies are (within the experimental error) identical to those known for pure silicon. For the 2% and 5% samples the 0_0 and 0_1 lines start to merge, and, although seen, it is impossible to assign their center of gravity for an Arrhenius plot analysis. As a result,

the numerical procedures used are unable to give parameters of these lines separately, and the Arrhenius plots in these cases have to be considered as actual plots of the 0Ge line as was done in the case of gold. For these two samples the enthalpies are considerable larger than for pure silicon, but again these values are not the best candidates for the reference levels.

Some problems with unambiguous assignment of the temperature shifts of the ''no germanium'' peaks and, as a consequence, the large standard deviation errors for the alloy coefficients makes any comparison of the data presented with the band offsets known from other experiments rather inconclusive. For the relaxed SiGe alloys (bulk) it has been concluded[22] from an analysis of the Schottky barrier heights for Si and Ge that most of the band-gap variation as a function of the alloy composition is due to a shift of the valence band. According to the data given in Ref. 22, if the alloy composition changes from 0% to 100% then the band gap shrinks by 0.45 eV while the top of the valence band moves up by 0.38 eV. According to our notation, this shift of the reference level related to the top of the valence band should be $(-0.43+0.05)$ eV. For the case of the gold acceptor level, if we assume that the level position of the 4Ge configuration in pure Ge measured by Pearton[19] is the correct value, then in reality the alloy coefficient of the 0Ge configuration is 0.24 eV smaller (in absolute value) than we have measured and equals $(-0.43-0.18)$ eV. If we assume that in the relaxed SiGe alloys the reference level follows the gold acceptor level (according to Langer and Heinrich[21]) then this value shows again that most of the band-gap decrease should be due to a shift of the top of the valence band and this shift should be much stronger than was concluded in Ref. 22. A similar analysis using the data of Pearton[19] for the platinum acceptor gives an even larger discrepancy with the data of Ref. 22. Finally, if one attempts to deduce the values of the alloy coefficients of the reference levels in SiGe one has to keep in mind that the band offsets in this alloy system are extremely sensitive to any strain in the crystal (see, e.g., Ref. 23 for details).

SUMMARY

High-resolution Laplace DLTS spectra for gold- or platinum-diffused SiGe samples show an alloy splitting that we associate with the alloy fluctuations in the proximity of the defect. For the case of platinum we can distinguish between the effect of the level splitting caused by alloying in the first and in the second shells of surrounding atoms. For the case of the gold acceptor only the effect from the first shell of atoms is observable but the manifestation of alloying in the second-nearest shell can be seen as line broadening, i.e., we cannot resolve the alloy splitting in the gold case. We have found that the electronic energy level is affected by alloying in the first-nearest neighborhood by a factor of 2–3 more than by alloying in the second-nearest shell. The absolute values of the energy differences obtained from the Arrhenius plots for different defect configurations agree with these inferred from the peak separations observed in the spectra. Quantitative differences in the spectra for the two different transition metals are due only to preferential experimental conditions (the higher resolution of the method) for the case of platinum than for gold. A clear preference for gold and platinum to enter substitutional Si sites adjacent to Ge has been revealed. This may be interpreted in terms of an enthalpy lowering as a result of the fact that both metals are able to replace the host silicon atom more easily in the substitutional position than the germanium atom.

ACKNOWLEDGMENTS

This work was supported in part by the Committee for Scientific Research Grant No. 8T11B00315 in Poland, the Danish National Research Foundation through the Aarhus Center for Atomic Physics (ACAP), the Danish Natural Scientific Research Council, the U.K. Royal Academy of Engineering, EPSRC, and European Community Grant No. CIPA-CT94-0172.

[1] P. Omling, L. Samuelson, and H. G. Grimmeiss, J. Appl. Phys. **54**, 5117 (1983).
[2] E. Calleja, F. Garcia, A. Gomez, E. Munoz, P. M. Mooney, T. N. Morgan, and S. L. Wright, Appl. Phys. Lett. **56**, 934 (1990).
[3] L. Dobaczewski and J. M. Langer, Mater. Sci. Forum **10-12**, 399 (1986).
[4] L. Dobaczewski, P. Kaczor, M. Missous, A. R. Peaker, and Z. R. Zytkiewicz, Phys. Rev. Lett. **68**, 2508 (1992).
[5] L. Dobaczewski, P. Kaczor, M. Missous, A. R. Peaker, and Z. R. Zytkiewicz, J. Appl. Phys. **78**, 2468 (1995).
[6] A. A. Istratov, O. F. Vyvenko, H. Hieslmair, and E. R. Weber, Meas. Sci. Technol. **9**, 477 (1998).
[7] L. Dobaczewski, P. Kaczor, I. D. Hawkins, and A. R. Peaker, J. Appl. Phys. **76**, 194 (1994).
[8] G. D. Watkins, M. Kleverman, A. Thilderkvist, and H. G. Grimmeiss, Phys. Rev. Lett. **67**, 1149 (1991).
[9] F. G. Anderson, R. F. Milligan, and G. D. Watkins, Phys. Rev. B **45**, 3279 (1992).
[10] F. Nikolajsen, P. Kringhøj, and A. Nylandsted Larsen, Appl. Phys. Lett. **69**, 1743 (1996).
[11] A. Mesli and A. Nylandsted Larsen, in *Defect and Impurity Engineered Semiconductors and Devices II*, edited by S. Ashok, J. Chevallier, K. Sumino, B. L. Sopori, and W. Goetz, Mater. Res. Soc. Symp. Proc. No. **510** (Materials Research Society, Pittsburgh, 1998), p. 89.
[12] A. Mesli, P. Kringhøj, and A. Nylandsted Larsen, Phys. Rev. B **56**, 13 202 (1997).
[13] A. Nylandsted Larsen, Mater. Sci. Forum **258-263**, 83 (1997).
[14] L. Dobaczewski, K. Gościński, K. Bonde Nielsen, A. Nylandsted Larsen, J. Lundsgaard Hansen, and A. R. Peaker, Phys. Rev. Lett. **83**, 4582 (1999).
[15] W. Schokley and W. T. Read, Jr., Phys. Rev. **87**, 835 (1952); S.

M. Sze, Physics of Semiconductor Devices (Wiley, New York, 1969).
[16] S. W. Provencher, Comput. Phys. Commun. **27**, 213 (1982); J. Weese, *ibid.* **69**, 99 (1992).
[17] A. A. Istratov and O. F. Vyvenko, Rev. Sci. Instrum. **70**, 1233 (1999).
[18] J. Weber and M. I. Alonso, Phys. Rev. B **40**, 5683 (1989).
[19] S. J. Pearton, Solid-State Electron. **25**, 305 (1982).
[20] See, e.g., *Heterojunction Band Discontinuities*, edited by F. Capasso and G. Margaritondo (North-Holland, Amsterdam, 1987).
[21] J. M. Langer and H. Heinrich, Phys. Rev. Lett. **55**, 1414 (1985).
[22] S. Tiwari and D. J. Frank, Appl. Phys. Lett. **60**, 630 (1992).
[23] F. Schäffler, Semicond. Sci. Technol. **12**, 1515 (1997).